

ARNF Coordinated Controller Design for SVC and TCSC in Power System

¹J. Sangeetha and ²P. Renuga

¹Department EEE, Ultra College of Engineering and Technology for Women, Madurai, India

²Department EEE, Thiagarajar College of Engineering, Madurai, India

Abstract: This study discusses and compares various co-ordinated controller design techniques for oscillation damping in nonlinear, complex power systems during transient disturbances. Multi-machine power systems are equipped with Thyristor Controlled Series Capacitor (TCSC) and Static Var Compensators (SVC) to enhance the stability of the systems. The damping controller co-ordinates measurement signals and control signals to control the TCSC and SVC devices. The Adaptive Recurrent based Neuro Fuzzy (ARNF) controller is employed to provide co-ordinated control signals to TCSC, SVC at each step depends upon the deviation in generator rotor speeds to enhance the stability of the Power System. To train NeuroFuzzy controller parameters, this study proposes the pheromone information updating in Ant Colony Optimization algorithms (ACO). The ACO algorithms based on Novel Pheromone Updating (ACO-NPU) scheme is employed to minimize the cost function and make the adaptive networks performance similar to a targeted training data. ARNF systems enable an extraction of rule-based knowledge from data and the introduction of a priori knowledge in the process of data analysis and system identification. The performance of proposed control strategy is evaluated in a three machine test system development in MATLAB for different scenarios. The nonlinear simulation results were compared with several modified PSO and continuous ACO algorithms. The results show that ACO with Pheromone Updating mechanism (ACO-NPU) handles continuous problems very well within a reasonable solution time without being trapped in local minimum.

Key words: Thyristor controlled series capacitor, static var compensator, adaptive recurrent neuro fuzzy control, ACO-NPU, India

INTRODUCTION

In fact of power system oscillations caused by large and complex interconnections power system stability is a major problem. Efforts have been done to enhance stability of the power system and damping the power system oscillations. Power System Stabilizers (PSS) is very effective controllers in enhancing the damping of low frequency oscillations by introducing additional control signals into the excitation controllers of the generators (Abido, 2000) Although, PSS suffers by a major drawbacks of serious variation in the voltage profiles and it may cause reduction of system stability under heavy disturbances. However, power electronic device known as Flexible Alternating Current Transmission System (FACTS) devices are effective in damping the inter-area oscillations and capable of handling the variations in voltage profile (Bian *et al.*, 2011). The co-ordination between various controllers are necessary to enhance the overall damping performance of power system (Chu and Tsai, 2008). Power systems are complex and nonlinear, so design of the controllers by linear methods cannot be able to maintain its stability in the event of large disturbances

(Juang and Chang, 2010). The advantages of fuzzy logic and neural network combined together constitute adaptive Neuro Fuzzy algorithm. The parameters of fuzzy logic controller are adjusted by learning ability of neural network in different scenarios to achieve a better performance over the conventional methods (Juang, 2004). The main objective of intelligent controller design is to avoid the dependence on experts and to get a control structure that does not need priori learning, i.e., the controller itself is able to learn about the controlled system and to adapt it on-line. Also, for dealing with dynamic systems, ARNF structure is a dynamic mapping network based on supervised learning which is more appropriate than the Neuro Fuzzy system (Kazemi *et al.*, 2007). This study examines the design of an auxiliary Adaptive Recurrent based Neuro Fuzzy (ARNF) co-ordinated SVC and TCSC controller to damp the power oscillations. Since, ARNF is an efficient and robust method for tuning the membership functions to reduce the measured output errors. An auxiliary ARNF based controller is developed to adapt the equivalent susceptance of the SVC and TCSC during the transient's conditions to improve the stability of the power system.

To improve the global searching ability of Neuro Fuzzy traditional learning structure (BP algorithm) ACO-NPU algorithm can be applied. The proposed ACO-NPU algorithm can efficiently tune the parameters of the Neuro Fuzzy network to meet the global solution.

MATERIALS AND METHODS

System model: The study system consists of three machines, three static loads and an inter-connecting network including transformers and transmission lines (LEE, 2001). The excitation system for the synchronous generator is the IEEE TYPE1 excitation system and the dynamic equations are based on nonlinear one axis model with a rotor reference. The small signal stability analysis is simulated to examine the location of the electromechanical modes. It is close to the imaginary axis of the complex plane necessities auxiliary devices to damp the oscillations. To improve voltage profile of generator bus 3, power flow in the transmission line between bus 2 and 3 SVC and TCSC devices inserted to the power system, respectively.

Static Var Compensator (SVC): Static var compensator is “a shunt-connected variable impedance type static var generator or absorber” whose output is adjusted to exchange capacitive or inductive current, so as to maintain or control desired voltages at the connected point of the electrical power system. The configuration of SVC is shown if Fig. 1. The Power system oscillations damping is implemented by super imposing the supplementary ARNF controller with automatic voltage control loop of SVC.

A block diagram of SVC control model for typical transient and oscillatory stability studies shown in Fig. 2. The model receives a voltage control signal (V_{con}) generated from auxiliary ARNF based controller and a susceptance reference signal B_{ref} generated from voltage regulator. The signals summed to produce an error signal ϵ fed into a first-order lag associated with the firing control and natural response of the SVC. Based on the SVC susceptance capability, the output of the regulator B_{SVC} has windup limits. A detailed description of the SVC control model is given by Lin *et al.* (2006).

Thyristor Controlled Series Capacitors (TCSC): The configuration of TCSC connected between nodes k and m in series with a line reactance jX_l and its equivalent circuit is shown in Fig. 3. In this study, the TCSC is treated as a variable capacitance.

Figure 4 shows a block diagram of a TCSC control model for typical transient and oscillatory stability studies. The model includes an input signal X_{con} and a

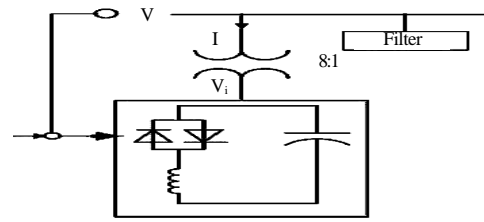


Fig. 1: Configuration of SVC

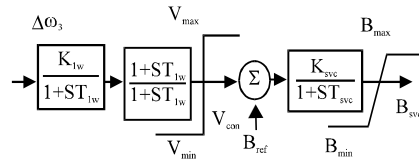


Fig. 2: SVC control model

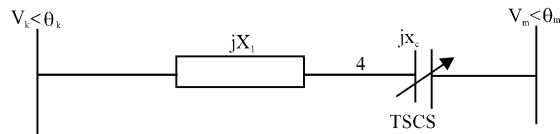


Fig. 3: Configuration of a TCSC

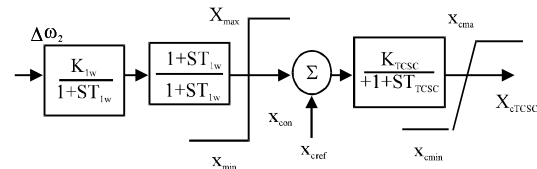


Fig. 4: TCSC control model

reference signal X_{ref} summed to produce an error signal ϵ , fed into a first-order lag associated with the firing control and natural response of the TCSC and is represented by a single time constant T_{TCSC} associated with it.

The study of the simple lower dimension three machine power system analysis easier the understanding of the design procedure and results. The multi-machine power system with SVC and TCSC is shown in Fig. 5 (Ratnaweera *et al.*, 2004) and bus data are given in Table 1.

Adaptive recurrent neurofuzzy control: The ARNF is a recurrent multi-layered connected network for determining the fuzzy inference system and it is efficient and robust method to reduce the measured output errors. The interesting features of the ARNF are that it has dynamic mapping ability, temporary memory, universal estimation and the fuzzy inference system. This study explains a fuzzy inference system implemented by using

Table 1: Multi-machine power system parameters and data

Generators	Load	Transformers	Transmission lines
f = 60 Hz, R _s = 2.8544e-1, X _d = 1.305, X' _d = 0.296, X'' _d = 0.252, X _q = 0.474, X' _q = 0.243, X'' _q = 0.18, T _d = 0.101 sec, T _{qo} = 0.1 sec, T' = 0.053 sec, P = 0.9748, d e1 Pe2 = 0.6094, Pe3 = 0.419	Load 2 = 7500 MW+1500 MVAR, Load 3 = Load4 = 25 W	ST1 = 4200 MVA, ST2 = ST3 = 2100 MVA, 13.8/500 kV, 60 Hz, R1 = R2 = 0.002, L1 = 0, L2 = 0.12, Rm = 500, Lm = 500	3-phase, L1 = 350 km, L2 = 50 km, L3 = 100 km, R1 = 0.0254 Ω km ⁻¹ R _o = 0.3864 km ⁻¹ , L1 = 0.9337e-3 H km ⁻¹ , L _o = 4.126e-3 H km ⁻¹ , 0 C1 = 12.74e-9 F km ⁻¹ , C _o = 7.751e-9 F km ⁻¹

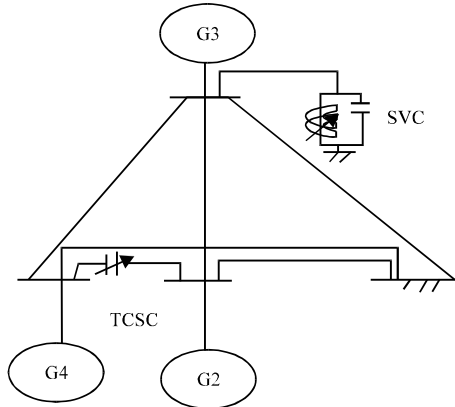


Fig. 5: Multimachine system

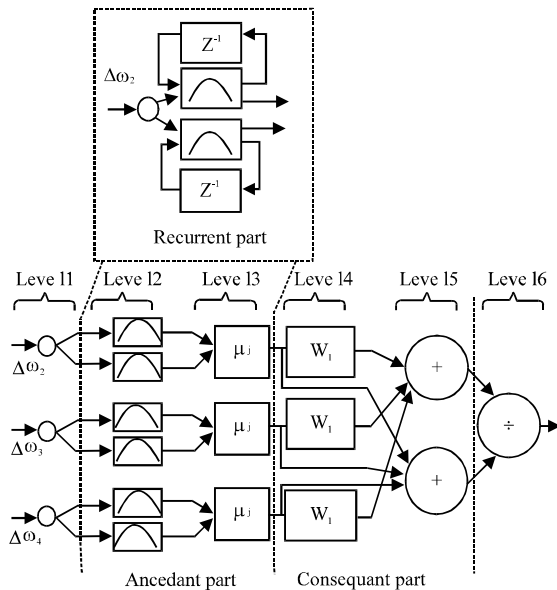


Fig. 6: Structure of the ARNF system

a multilayer recurrent neural network called an ARNF shown in Fig. 6. The overall control algorithm is shown in Fig. 7. The ARNF structure has 3 input variables, 5 nodes for each input variable, 8 output nodes, 5×3 rule nodes. These six layers in ARNF system represents following functions. Layer I accepts input variables $\Delta\omega_2, \Delta\omega_3, \Delta\omega_4$. Its nodes represent input linguistic variables. Layer II is used to estimate the terms of the linguistic variable in

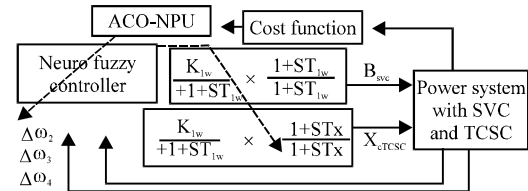


Fig. 7: The structure of the ARNF coordinated controller

Gaussian membership function. Nodes at Layer III denote fuzzy rules. Links before the Layer III represent the antecedent part of the rules and the consequent part of the rule nodes characterized by the links after Layer III. Layer IV represents the weights of neural systems and Layer V and VI represent the defuzzification of the Neuro Fuzzy system.

ARNF layered structure: A fuzzy logic system normally accesses its input and output of the network data in the shape of a fuzzy algorithm, which consists of a fuzzy linguistic and the ‘min’ rule has the form of: R: If $\Delta\omega_2$ is A_{1i} and $\Delta\omega_3$ is A_{2i} and $\Delta\omega_4$ is A_{3i} . Then, K_{1w} is B_{1i} , T_{1w} is B_{2i} , T_{11} is B_{3i} , T_{12} is B_{4i} , K_{2w} is B_{5i} , T_{2w} is B_{6i} , T_{21} is B_{7i} , T_{22} is B_{8i} where, $i = 1, \dots, R$ (no of rules). The structure for the ARNF network has six layers and each layer performs the function to the incoming signals.

Layer I: This layer is the input layer, accepts the input values and transmits it to the next layer.

Layer II: In this layer the fuzzification process is performed and neurons represent fuzzy sets used in the antecedents’ part of the linguistic fuzzy rules. The outputs of the layer II are the values of the membership functions, μ_{ij} . The membership of i th input variable to j th fuzzy set is defined by Gaussian membership function and be represented as membership function: Degrees of membership function of layer II:

$$\eta_{ij}(k) = e^{-\frac{(I_i(k) - g_{ij})^2}{S_{ij}^2}}$$

Where:

- I_i = The input variable, k is the number of input variable
- g_{ij}, s_{ij} = The mean and variance of the Gaussian membership function

Input variable, $I_i(k) = \epsilon^1(k) + \epsilon^2(k)$; $k = 1, 2, 3$ no of input variable where, $\epsilon^1(k)$, $\epsilon^2(k)$ is the input to first layer and second layer. Input to second layer:

$$\epsilon^2(k) = \eta_{ij}(k-1) \times \Omega_{ij}(k)$$

Where:

$\eta_{ij}(k-1)$ = The previous value of membership function
 Ω_{ij} = The linkage weight in the feedback unit

The difference between the Neuro Fuzzy and recurrent Neuro Fuzzy system is, the later one has the memory terms to store the previous information of the network.

Layer III: This layer is called as fuzzy inference layer and each node represents a fuzzy rule. The firing strength of each rule (μ_{ij}) is the output value of the layer and calculated by min operator.

Layer IV: This layer represents the hidden weights of the ARNF system.

Layer V and VI: These layers operate the defuzzification process, i.e.,

$$u = \frac{\sum_{i=1}^m \mu_{ij} w_{ip}}{\sum_{i=1}^m \mu_{ij}}$$

where, u is the output for the entire network. After estimating the output value of the ARNF system, the training of the network starts and w_{ip} are the weights between the neurons of III and IV layers and $p = 1, 2, \dots, n$; 'n' is the number of classes.

Learning of update parameters: The ARNF learning process is performed to minimize the error input and output values by adjusting network parameters. The gradient descent method is used to adjust the values of weights w_{ip} and mean g_{ij} and variance s_{ij} of the membership function ARNF. Gradient descent method is used to minimize the error $E(K)$ between the actual output value of the system ($Y(K)$) and the desired value $Y_d(k)$. The back propagation learning algorithm is used for updating parameters of the ARNF system. The error expression for each layer is first calculated by recursive functions of the chain rule and then the parameters in the corresponding layers are adjusted. The updated of the parameter can be expressed as:

$$w_{ip}(k+1) = w_{ip}(k) - \alpha \frac{\partial E}{\partial w_{ip}}$$

where, α shows the learning rate. The chain rule for the w_{ip} can be expressed as:

$$\frac{\partial E}{\partial w_{ip}} = \frac{\partial E}{\partial y} \times \frac{\partial y}{\partial u} \times \frac{\partial u}{\partial w_{ip}}$$

Similarly, the remaining parameters g_{ij} , S_{ij} , Ω_{ij} updated. The above equations given the required change in updated of the parameters in ARNF network. In ACO-NPU, an online-rule-generation method is proposed to generate both rules and determines their proper initial locations in the input space (i.e., proper initial-antecedent-part parameters).

Ant colony optimization based on a novel pheromone updating scheme:

One of the population-based metaheuristic technique, Ant Colony Optimization (ACO) finds good path through graphs that can be used to find global minimum. In ACO, a set artificial ants incrementally build solutions by moving on the graph for a given optimization problem. These artificial ants communicate only by laying pheromone and the more pheromone in a particular part is the more desirable part to the ants. This is the way how the ants find the solutions. The purpose of the novel pheromone update rule is to encourage ants to search for paths in the vicinity of the best tour found so far so as to converge to a common path.

Firstly, the solution archive is initialized. Then, at iterations, number of solutions is constructed by the ants according to pheromone values. At the last step, the solution archive and pheromone values are updated. In ACO, artificial ants build a solution to a combinatorial optimization problem, the steps explained in detail as follows. First, each instantiated decision variable is called a solution component and denoted by solution archive ($x_{kminial}$, $k = 1, 2, \dots$ archive size) and $f(x_{kminial})$ is computed. A pheromone trail value is associated with the set of all possible solution components. Pheromone values allow the probability distribution of different components of the solution to be modeled. Pheromone values are used and updated by the ACO algorithm during the search.

Then, new pheromone values are computed for the last selected solutions (remaining solutions). Up to this step, actually a local search is performed among the candidate solutions. Then, in order to approximate the best solution at the end of the each iteration, Euclidean distances of candidate solutions to the best known solution are computed in Eq. 1. In other words, differences between minimum objective function value of $f(f_{min})$ and the other candidate function (f) values are computed with Eq. 1. Euclidean distances:

$$E_i = f_i - f_{min}$$

In order to define continuous variables, Gaussian functions were selected. Gaussian function is used to compute probabilities by using E_i :

$$G_i = e^{-\frac{E_i^2}{2t}} \quad (2)$$

The parameter t in Gaussian function denotes standard deviation. Numerous experiments were performed to determine parameter t and in this problem t is set to 0.005. In order to determine with percentiles of how many ants which would go into the best candidate solution, normalization is made with Eq. 3. Normalized values are obtained from Gaussian function:

$$\tau_i = \frac{G_i}{\sum_{i=z}^n G_i} \quad (3)$$

where, τ_i is pheromone trail value of the solution. To generate new solutions, each ant chooses a reference point according to pheromone values of solutions. For example, consider five artificial ants were searching the solution and the pheromone values of second artificial ant is computed as 0.3781 at the end of the iteration, then 38% of ants (i.e., 2 ants) approximately will use 2nd solution as a reference point to produce new solutions. Therefore, the 5 paths are converged to four path, that is the way to converge to a better solution to generate new solutions:

$$x_m^1 = x_{m-1}^1 \pm dx \quad (4)$$

where, x_m^1 is solution vector of the l th ant at iteration m , x_{m-1}^1 is the selected best solution in solution archive (reference point) according to pheromone value at iteration $m-1$ for l th ant and dx is a vector generated randomly from $(-\beta, \beta)$ range to determine the length of jump. Generated new solutions by Eq. 4 is added to existing archive and the size of archive is increased to $l+m$ (archive size+ant size). Because archive size must be kept as l , archive size is updated. This process is iterated until number of maximum iteration reached (m). At the end of the each iteration, quantity of pheromone is updated. To simulate the evaporation process quantity of pheromone is reduced with the following Eq. 5:

$$\beta_m = 0.9 \times \beta_{m-1} \quad (5)$$

By experiments, the co-efficient of evaporation is set as 0.9 and if the co-efficient of evaporation is kept smaller or >0.9 , there is a possibility of being trapped in local optimum.

RESULTS AND DISCUSSION

To justify the performance of proposed supplementary control strategy for SVC, the nonlinear simulations were carried out in a multi-machine power system. To guarantee the efficiency and robustness of the proposed ARNF control approach, large and small perturbances are added to the power system during simulations. They are categorized into two cases as discussed under the following section.

Case 1: To examine the effectiveness of the proposed ARNF control strategy, the controller training is performed by applying small incremental torque 0.1 PU to G2, G3, G4 at 0.1 sec and disappeared at 0.3 sec. To compare the results, the cost function (Lu *et al.*, 2013) is considered. The dynamic response of speed deviation and angles for G2, G3, G4 shown in Fig. 8a-c. The speed deviation for G2, G3, G4 shown in Fig. 8a-c and the rotor angle deviation for G2, G3, G4 shown in Fig. 8d-f reveals that in the first swing, the overshoot of the system is decreased very much with ARNF which shows its improved performance during the transient state. The average cost and standard deviation is smaller when ACO-NPU technique is employed. Also t-test is used for statistical analysis to evaluate the difference between ACO-NPU and other algorithms. To prove the efficacy of the proposed ACO-NPU approach, several modified PSO and continuous ACO algorithms were applied to the same evolutionary fuzzy lead lag controller. To enhance convergence to global optimum solution the modified PSO algorithms such as Hierarchical PSO with Time varying Acceleration Co-efficient HPSO-TVAC (Paserba *et al.*, 1995) is used. A hybrid of GA-PSO (HGAPSO) finds a better solution without trapping in local maximum and an improved PSO algorithm (Socha and Dorigo, 2008) to improve the capability of global searching. The comparisons include the modified continuous ACO algorithm with different coefficients $q = 0.01$ and $q = 10$ (Lin *et al.*, 2009; Yuan and Fang, 2009), RACACO, ACACO (Lu *et al.*, 2013). Table 2 shows learning performance of ACO-NPU, various modified PSO and evolutionary fuzzy lead lag controller technique. The result indicates that the average cost value C is smaller for the ACO-NPU algorithm than the other algorithms.

Case 2; (three line to ground fault): To examine the effectiveness of the proposed ARNF control strategy, 3 cycle three line to ground fault is applied on transmission line L3 at $t = 0.2$ sec between buses 1 and 2.

The fault is self-cleared at $t = 0.3$ sec. Figure 9a-c shows the inter-area speed deviation of G2, G3, G4 and

Table 2: Learning performance of ACO-NPU, various modified PSO and evolutionary fuzzy lead lag controller

Algorithms	HPSO-TVAC (Ratnaweera <i>et al.</i> , 2004)	HGAPSO (Juang, 2004)	IPSO (Lin <i>et al.</i> , 2009)	ACOR _R (q = 0.01) (Socha and Dorigo, 2008)	ACOR _R (q = 0.01) (Socha and Dorigo, 2008)	RACACO (Juang and Chung, 2010)	ACACO (Chun-Feng <i>et al.</i> , 2013)	ACO-NPU
Average cost	0.047487	0.048821	0.047504	0.04802	0.04743	0.04669	0.0465	0.0464
STD	0.00076	0.000968	0.000549	0.001445	0.00067	0.00044	0.00024	0.00018
t-value	6.357	9.587	9.07	5.636	7.164	1.989	1.347	-

Table 3: SAD values of the generators for case (2)

Lead key	$ \Delta\omega _2$	$ \Delta\omega _3$	$ \Delta\omega _4$	$ \Delta\delta _2$	$ \Delta\delta _3$	$ \Delta\delta _4$
Lead-lag	0.000192	0.000850	0.000872	0.46732	0.194235	0.464231
Fuzzy-lead lag (Lu <i>et al.</i> , 2013)	0.000156	0.000450	0.000578	0.36689	0.121561	0.304135
ACO-NPU based fuzzy lead lag	0.000130	0.000030	0.000540	0.35460	0.101234	0.293421

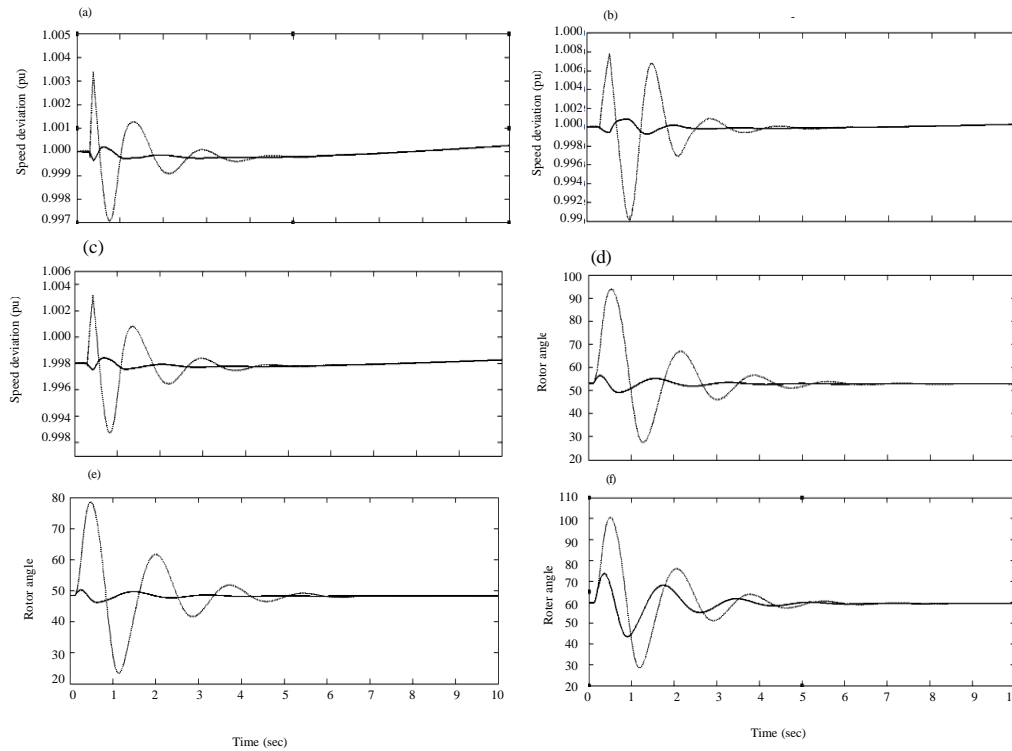


Fig. 8: a-d) Dynamic response of speed deviation and angles in G2; b, e) Dynamic response of speed deviation and angles in G3; c, f) Dynamic response of speed deviation and angles in G4 using ARNF control lead lag controller for case 1

Fig. 9a-b shows the inter-area rotor angle deviation of the perturbed system for G2, G3, G4. The post fault system response in steady state region is oscillatory with lead lag controller and in case of fuzzy lead lag controllers oscillation can be observed with ACO-NPU algorithm as shown in Fig. 9a-f reveals that in the first swing, the overshoot of the system is decreased very much with ACO-NPU which shows its improved performance during the transient state. The settling time of proposed control is also reduced very much as compared to other control strategies. The control effort provided by the respective control schemes is shown in Fig. 9. It can be seen from

result that when the fault occurs in the system, then the ARNF increases its control effort to bring the system to a stable equilibrium point and to damp the oscillations quickly. For quantitative analysis Sum of Absolute Deviation (SAD) values for G2, G3, G4 are tabulated in Table 3.

The lead lag controller damps the oscillation but the fuzzy lead lag controller based on ACO-NPU technique damps the oscillations very efficiently. Table 3 shows the SAD values of the generators are lesser when using ACO-NPU fuzzy lead lag controller over the other methods.

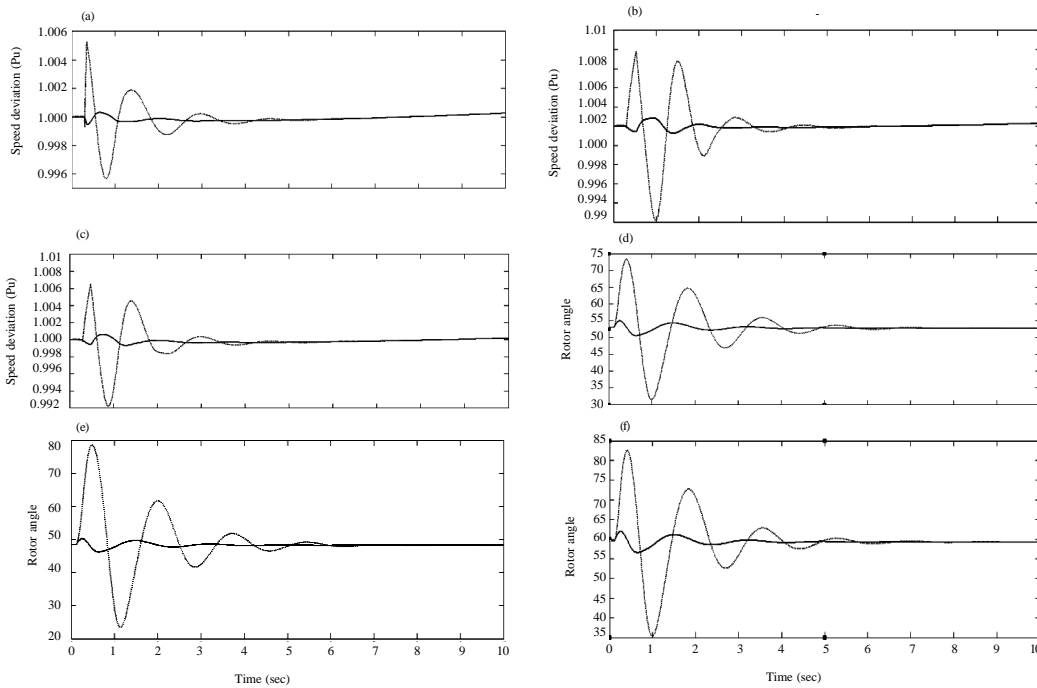


Fig. 9: a, d) Dynamic response of speed deviation and angles in G2; b, e) Dynamic response of speed deviation and angles in G3; c, f) Dynamic response of speed deviation and angles in G4 using ARNF control lead lag controller for case (2)

CONCLUSION

This study concludes the co-ordinate control strategy of SVC, TCSC Facts devices for damping the oscillations. The simulation results verify the oscillation damping ability of the ACO-NPU based fuzzy lead lag control approach. The ACO-NPU based fuzzy lead lag control approach simplifies the design of lead lag controller and effectively improves the system dynamics. The comparisons with various modified PSO and ACO algorithms verify the advantage of ACO-NPU technique.

REFERENCES

Abido, M.A., 2000. Robust design of multimachine power system stabilizers using simulated annealing. *IEEE Trans. Energy Convers.*, 15: 297-304.

Bian, X.Y., C.T. Tse, J.F. Zhang and K.W. Wang, 2011. Coordinated design of probabilistic PSS and SVC damping controllers. *Int. J. Electr. Power Energy Syst.*, 33: 445-452.

Chu, C.C. and H.C. Tsai, 2008. Application of lyapunov-based adaptive neural network UPFC damping controllers for transient stability enhancement. *Proceeding of the conference Power and Energy Society General Meeting-Conversion and Delivery of Electrical Energy in the 21st Century, 2008 IEEE. July 20-24, 2008, IEEE, Pittsburgh, PA.*, pp: 1-6.

Juang, C.F., 2004. A hybrid of genetic algorithm and particle swarm optimization for recurrent network design. *IEEE Trans. Syst. Man Cybern. Part B: Cybern.*, 34: 997-1006.

Juang, C.F. and P.H. Chang, 2010. Designing fuzzy-rule-based systems using continuous ant-colony optimization. *Fuzzy Syst. IEEE. Trans.*, 18: 138-149.

Kazemi, A., M.J. Motlagh and A.H. Naghshbandy, 2007. Application of a new multi-variable feedback linearization method for improvement of power systems transient stability. *Int. J. Electr. Power Energy Syst.*, 29: 322-328.

LEE, Y.S., 2001. Decentralized suboptimal control of power systems with superconducting magnetic energy storage units. *Int. J. Power Energy Syst.*, 21: 87-96.

Lin, F.J., P.H. Shen, S.L. Yang and P.H. Chou, 2006. Recurrent radial basis function network-based fuzzy neural network control for permanent-magnet linear synchronous motor servo drive. *Magn. IEEE.*, 42: 3694-3705.

Lin, F.J., L.T. Teng, J.W. Lin and S.Y. Chen, 2009. Recurrent functional-link-based fuzzy-neural-network-controlled induction-generator system using improved particle swarm optimization. *Ind. Electr. IEEE. Trans.*, 56: 1557-1577.

- Lu, C.F., C.H. Hsu and C.F. Juang, 2013. Coordinated control of flexible AC transmission system devices using an evolutionary fuzzy lead-lag controller with advanced continuous ant colony optimization. *Power Syst. IEEE. Trans.*, 28: 385-392.
- Paserba, J., N. Miller, K. Palm, E. Laesen and R. Piwko, 1995. A Thyristor controlled series compensation model for power System stability analysis. *IEEE. Trans. Power Delivery*, 10: 1471-1478.
- Ratnaweera, A., S.K. Halgamuge and H.C. Watson, 2004. Self organizing hierarchical particle swarm optimizer with time varying acceleration coefficients. *IEEE Trans. Evol. Comput.*, 8: 240-255.
- Socha, K. and M. Dorigo, 2008. Ant colony optimization for continuous domains. *Eur. J. Oper. Res.*, 185: 1155-1173.
- Yuan, S.Q. and D.Z. Fang, 2009. Robust PSS parameters design using a trajectory sensitivity approach. *Power Syst. IEEE. Trans.*, 24: 1011-101